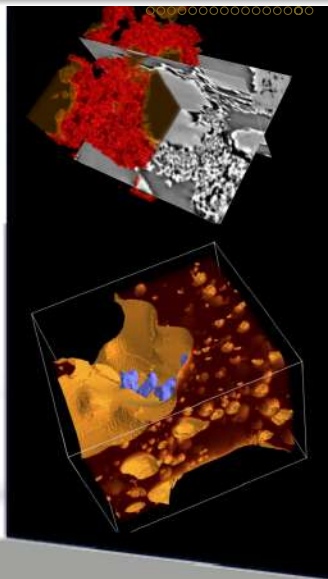


In-situ tomographic imaging of glasses and melts

Emmanuelle Guillard
Joint Unit CNRS/Saint-Gobain SVI

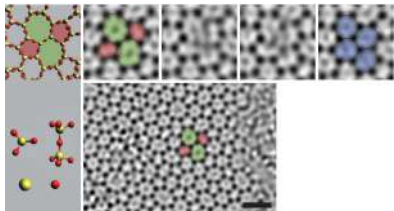


Imaging glasses and melts

Looking at heterogeneous systems



not much to be seen !



[Huang et al., Science 2013]

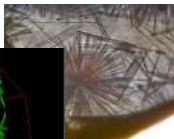
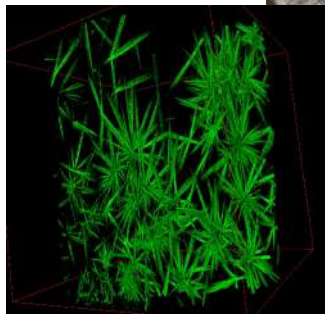
HRTEM of 2D silica

Not in this talk !

Imaging glasses and melts

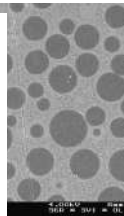
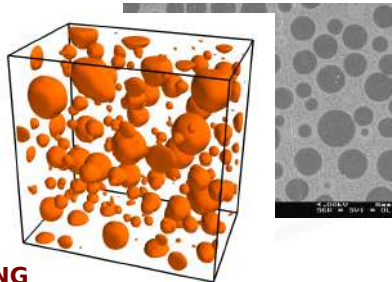
Looking at heterogeneous systems

CRYSTALLIZATION



Sophie Schuller, Elise Régnier (CEA)

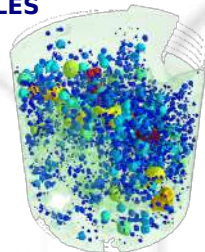
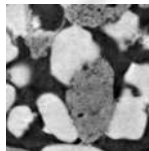
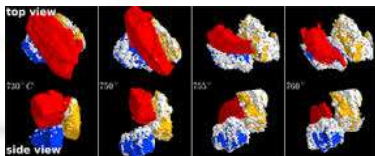
PHASE SEPARATION



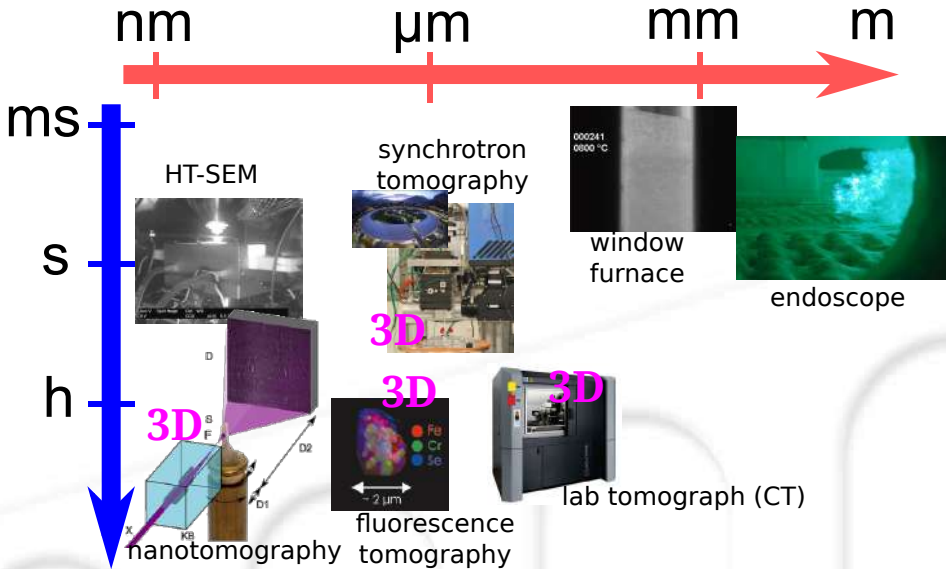
IMAGING
PHASES

BUBBLES

GLASS-FORMING BATCHES



Different imaging modalities : speed vs. resolution



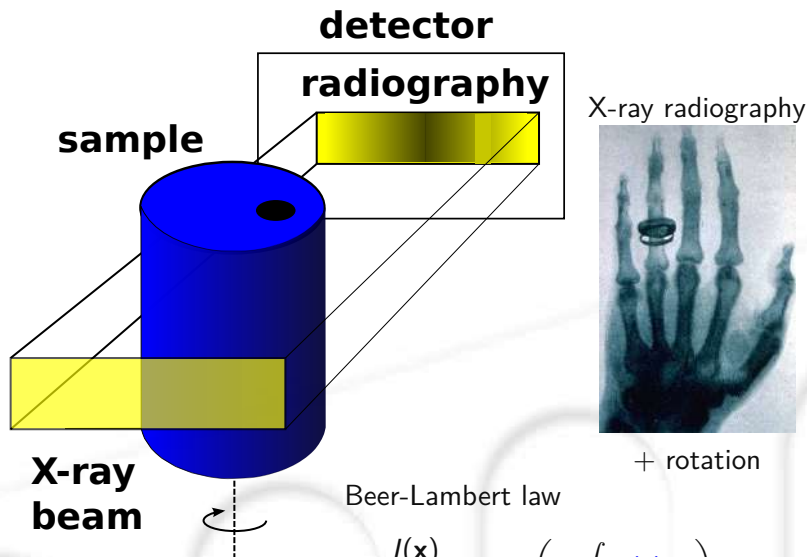
1 In-situ tomography

2 Applications

Phase separation

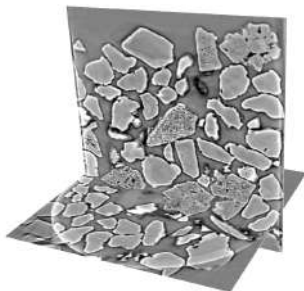
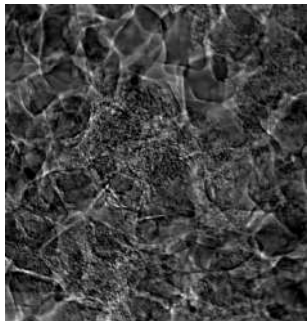
Glass reactive melting : reaction paths between granular raw materials

Principle of synchrotron microtomography

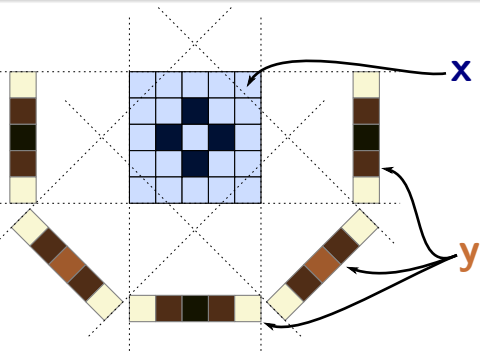


$$\frac{I(\mathbf{x})}{I_0(\mathbf{x})} = \exp\left(-\int \mu(s) ds\right)$$

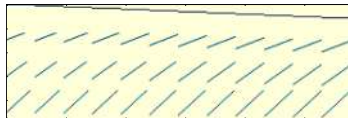
Obtaining 3-D absorption maps from 2-D radiographies



Tomographic reconstruction : an inverse problem



$$y = Ax$$



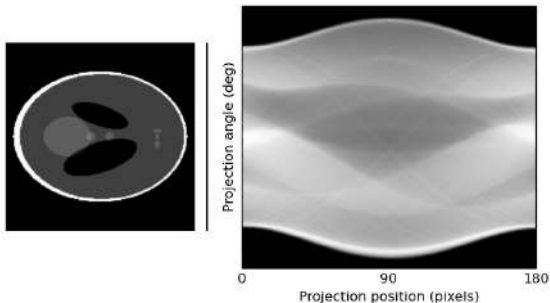
$$y \in \mathbb{R}^n, \quad A \in \mathbb{R}^{n \times p}, \quad x \in \mathbb{R}^p$$

$n \propto$ number of projections

p : number of pixels in reconstructed image

We want to find x knowing A and y

Principle of synchrotron microtomography



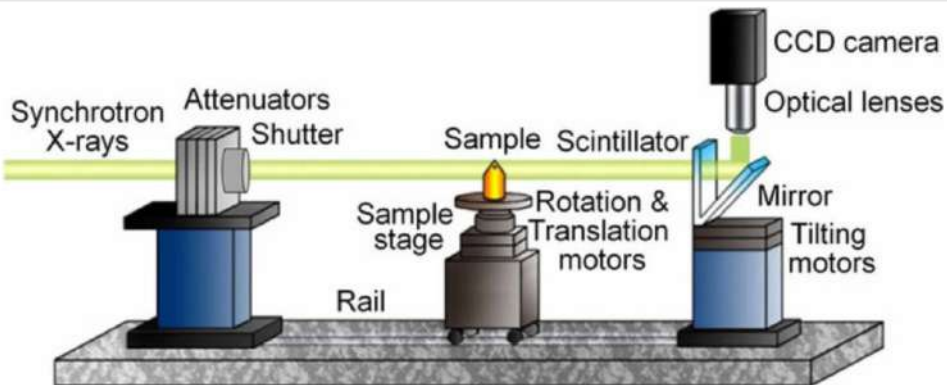
Unknown data :
One horizontal cut through
sample

[Slaney and Kak, 1988]

Measured data :
One line of the camera, at all
projection angles



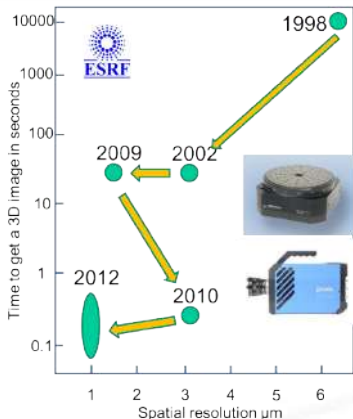
Synchrotron microtomography



Credit : Francesco De Carlo, APS

- **Spatial** resolution limited by
 - optical lenses (diffraction)
 - scintillator (blurring)
- **Time** resolution limited by
 - X-ray photon flux
 - camera sensitivity, . . .

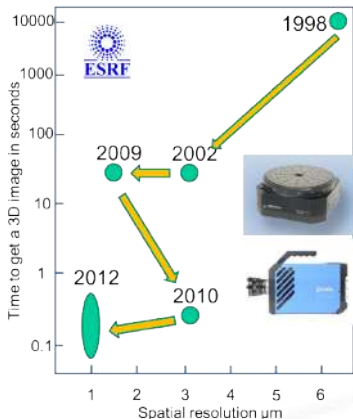
In-situ acquisition is possible in 3-D



Ultrafast 3-D imaging
available at ESRF, APS, SLS

Acquisition rate depends a lot
on sample (absorption, dose
sensitivity, ...)

In-situ acquisition is possible in 3-D

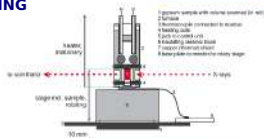


Ultrafast 3-D imaging
available at ESRF, APS, SLS

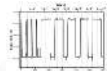
Acquisition rate depends a lot
on sample (absorption, dose
sensitivity, ...)

A variety of in-situ setups are available

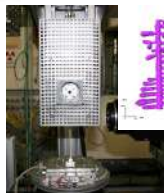
MECHANICAL LOADING



HUMIDITY AND HEATING CONTROL



Dehydration of Gypsum



FURNACES

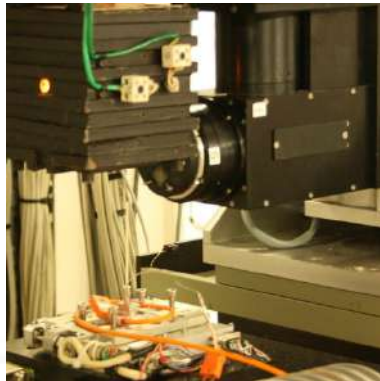


Heating devices

Chamber furnaces



Simap furnace, 300-800°C
[Terzi et al., 2010]



Ecole des Mines furnace, 700-1500°C
[Limodin et al., 2009]

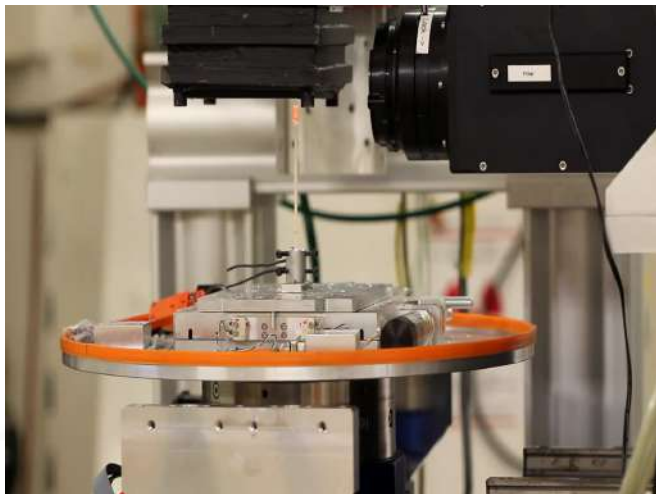
Advantages

homogeneity of temperature field

Drawbacks

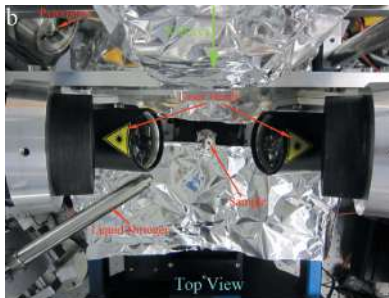
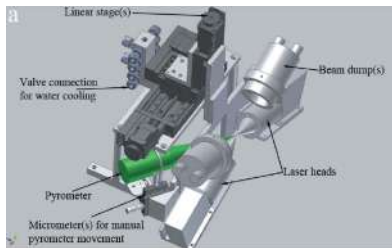
slow quenching
bulky

Continuous rotation for ultrafast acquisition



Heating devices

Laser heating



Tomcat beamline, SLS PSI [Fife et al., 2012]

Advantages

fast heating

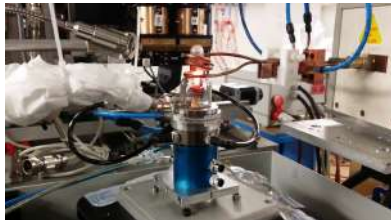
minimal space requirement

Drawbacks

homogeneity of temperature field

Heating devices

Induction heating



Advantages

fast heating
controlled atmosphere

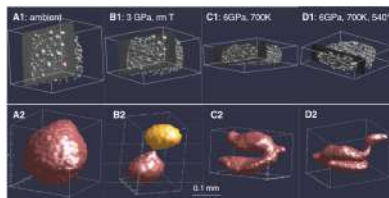
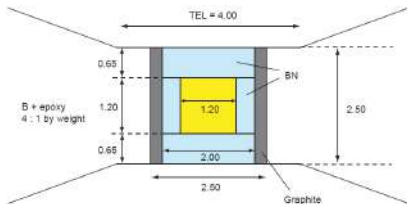
Drawbacks

homogeneity of temperature field

High-temperature environments

High temperature and high pressure

Argonne synchrotron (APS)



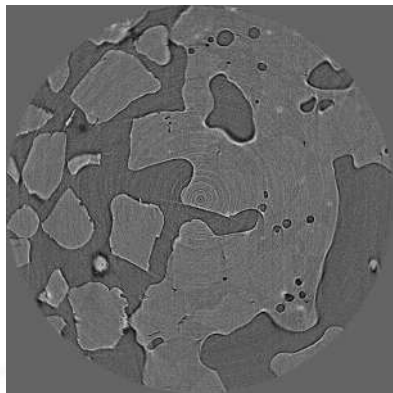
connectivity of Fe-Ni-S
inclusions in a silicate (olivine)
matrix

[Wang et al., 2005, Lesher et al., 2009, Wang et al., 2009,
Wang et al., 2011]

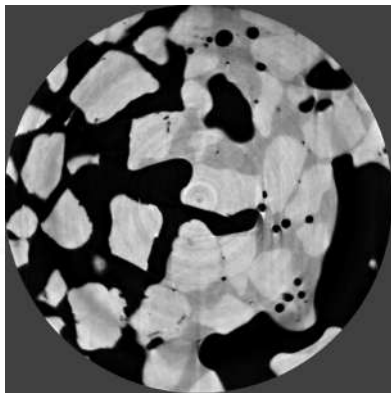
Absorption and phase contrast

Good spatial coherence @ ESRF \rightarrow phase can be reconstructed

$$n = 1 - \delta + i\beta$$



Absorption reconstruction

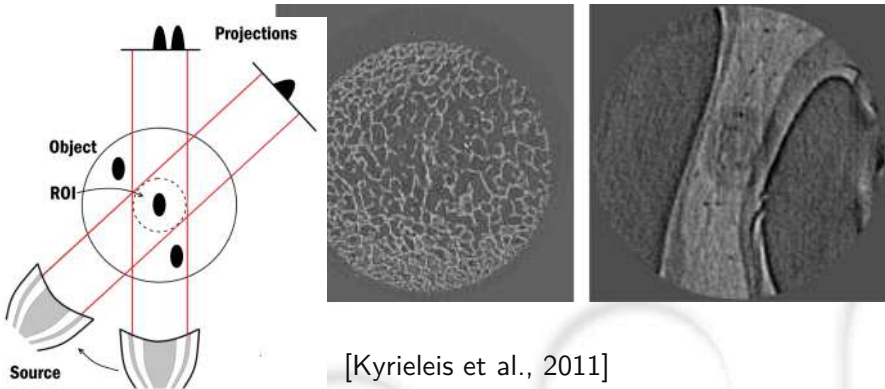


(approximate) phase
reconstruction

[Paganin et al., 2002, Weitkamp et al., 2012]

Local tomography

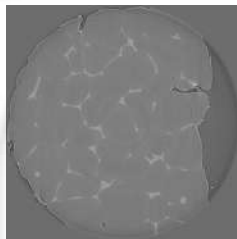
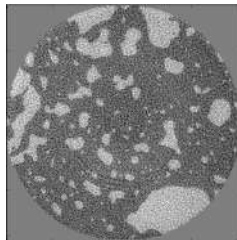
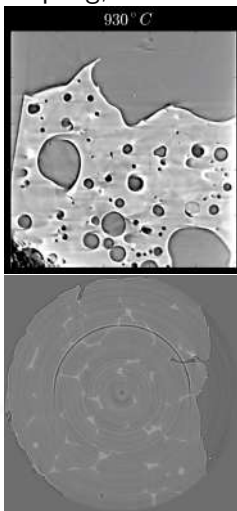
Possible to zoom into the sample



[Kyrieleis et al., 2011]

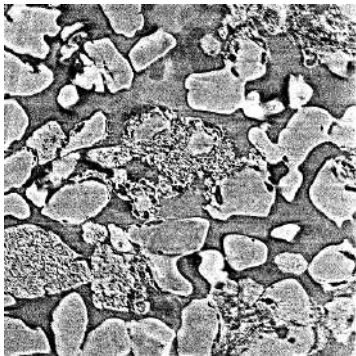
Artifacts

Multiple sources of artifacts : sample motion, sensor non-linearities, undersampling, etc.



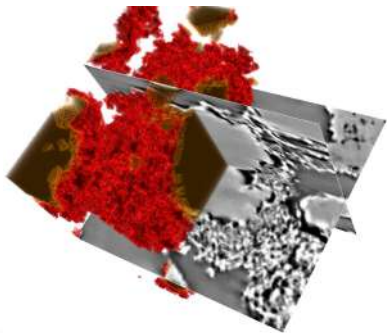
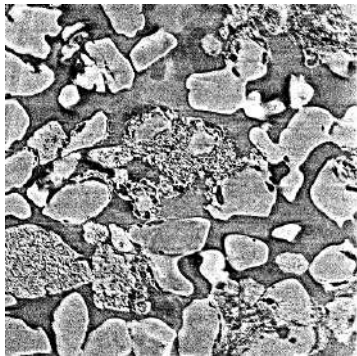
Images from Limodin, Salvo, Cloetens

Heavy-duty image processing



- Large datasets : 100 Go for one experiment !
- Noisy images : tradeoff between speed and quality
- Longer to process the images than to acquire them !

Heavy-duty image processing



- Large datasets : 100 Go for one experiment !
- Noisy images : tradeoff between speed and quality
- Longer to process the images than to acquire them !

1 In-situ tomography

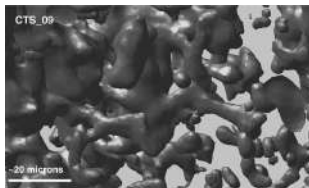
2 Applications

Phase separation

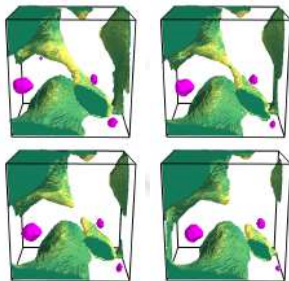
Glass reactive melting : reaction paths between granular raw materials

Advantages of (in-situ) X-ray tomography

- 3-D images \Rightarrow connectivity, topology
- more statistics on objects/particles
- non-destructive : follow the same sample
- time resolution : don't miss important events

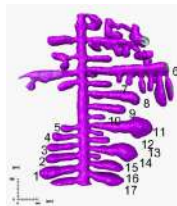


[Watson and Roberts, 2011]



[Bouttes et al., 2015]

Tomography has been used for a long time in metallic alloys



163s, 626°C, 0.19



219s, 623°C, 0.29



275s, 620°C, 0.37



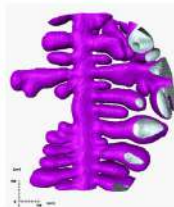
329s, 618°C, 0.42



384s, 615°C, 0.46



440s, 612°C, 0.52



495s, 609°C, 0.56



551s, 606°C, 0.58

Mechanisms of dendritic growth in Al-Cu [Limodin et al., 2009]

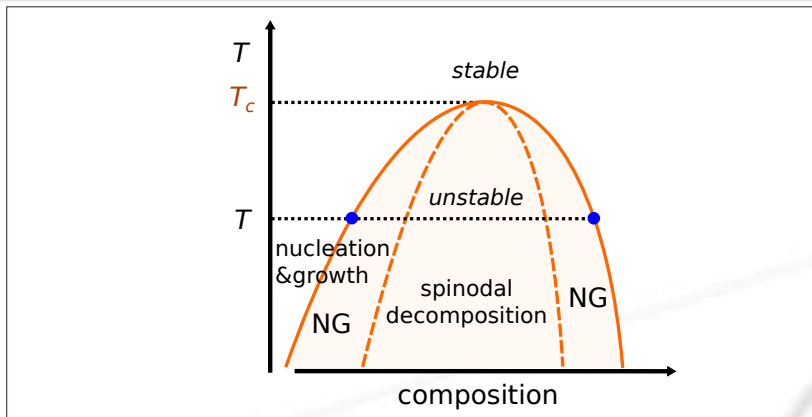
1 In-situ tomography

2 Applications

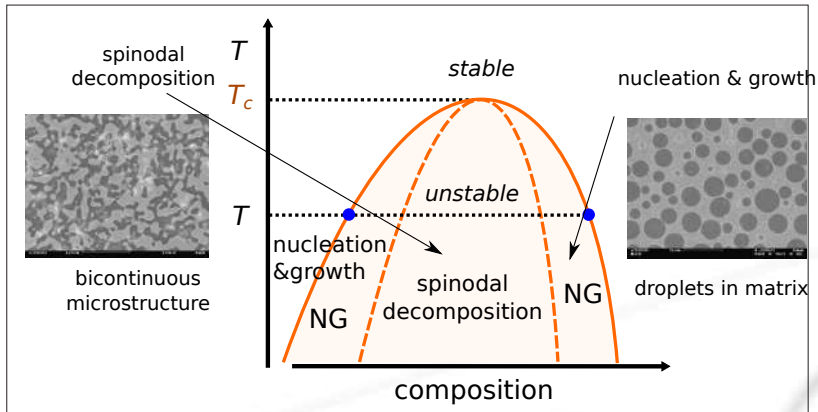
Phase separation

Glass reactive melting : reaction paths between granular raw materials

Principles of phase separation

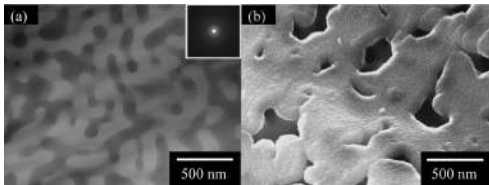


Principles of phase separation



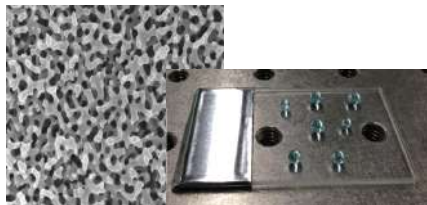
- No 1-to-1 correspondence between thermodynamic regime (SD, NG) and microstructure of phases
- Silicate melts : phase separation possible in stable or metastable liquids

Porous membranes: Vycor



Suzuki et al. 2008

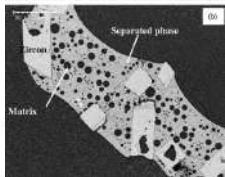
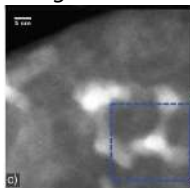
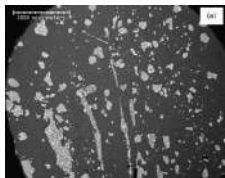
Super-hydrophobic porous films



Aytug et al. 2013

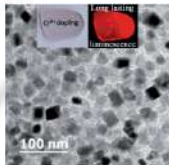
Nuclear waste glasses

Dargaud et al. 2012



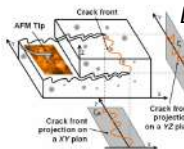
Martineau et al. 2010

Glass ceramics



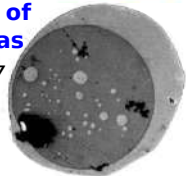
Model materials for crack propagation

Dalmas et al. 2008



Microstructure of basaltic magmas

Veksler et al. 2007



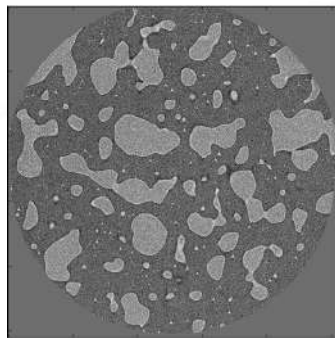
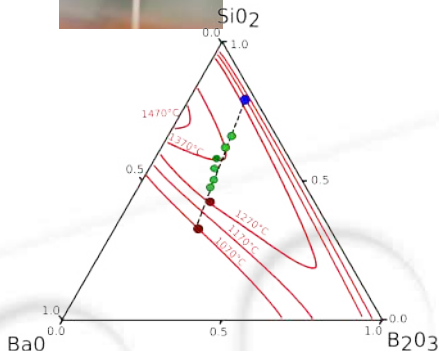
Luminescent glass

Chenu et al. 2014

In-situ experiments on ID19, ESRF - David Bouttes

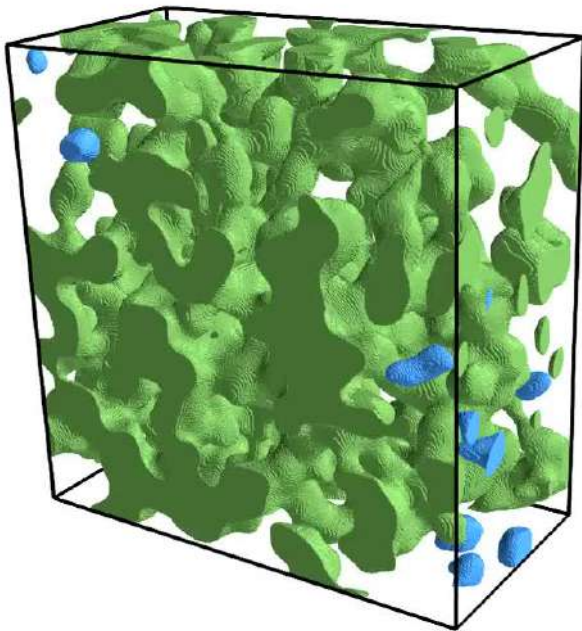


- pink beam 35 keV (barium is very absorbing !)
- pixel size 0.55 or 1.1 μm
- acquisition times 5s - 1min
- local (ROI) tomography
- temperatures : 1000 - 1300° C

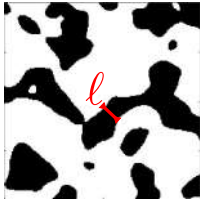


FOV : 2mm

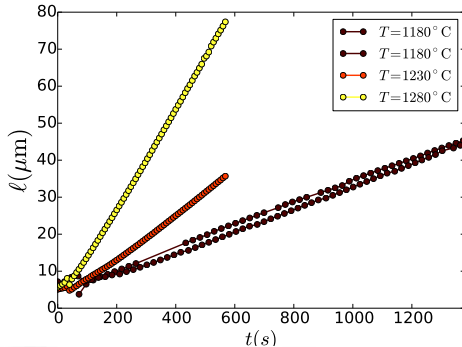
Coarsening : $\phi \leq 0.5$ case



Evolution of characteristic length



$$l = \frac{\mathcal{V}}{S}$$

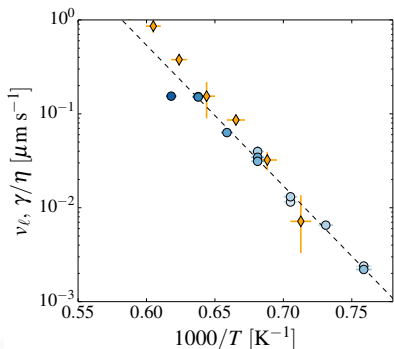
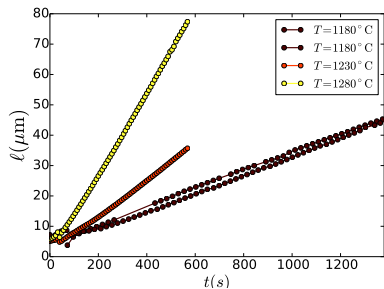


■ linear evolution with time

■ coarsening rate increases with temperature

\Rightarrow is hydrodynamic flow the dominant mechanism ?

Evolution of characteristic length

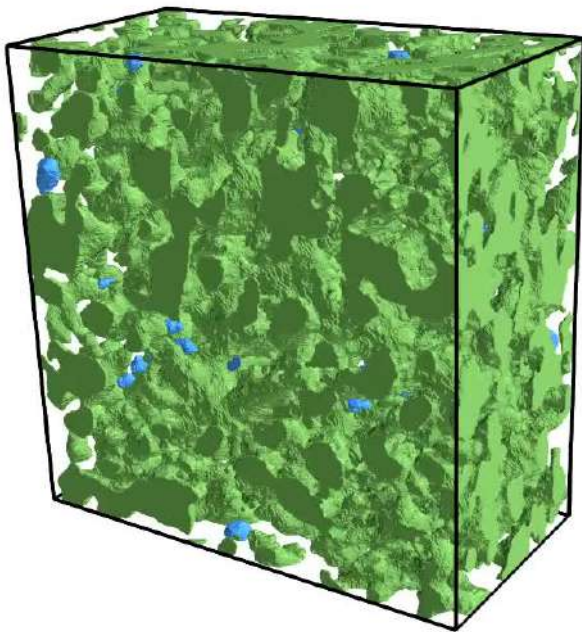


Evolution consistent with viscous coarsening :

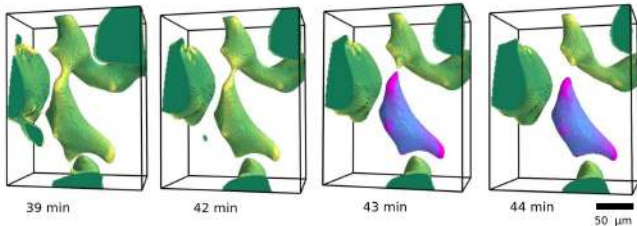
$$\dot{l}(t) \simeq \frac{\gamma}{\eta}$$

[Bouttes et al., 2014, Bouttes et al., 2015]

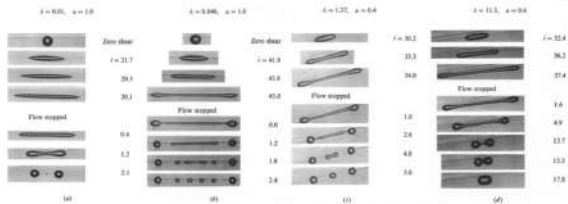
Coarsening and fragmentation



Close-up on domain break-up



Only the barium-rich phase breaks up in domains



- Viscous filaments tend to retract
- Less viscous filaments tend to break

[Stone and Leal, JFM 1989]

1 In-situ tomography

2 Applications

Phase separation

Glass reactive melting : reaction paths between granular raw materials

Reactive melting of glass raw materials

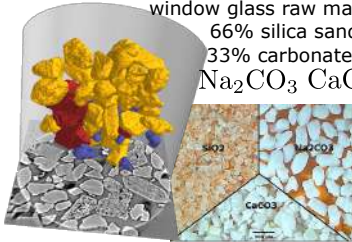
Soda-lime silica glass - William Woelffel

window glass raw materials:

66% silica sand

33% carbonates

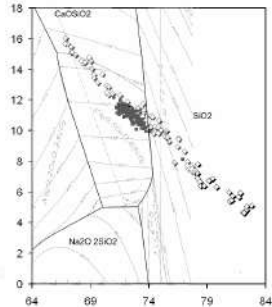
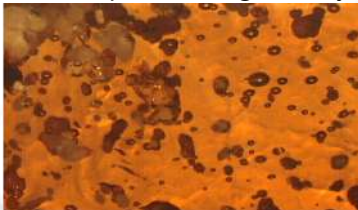
Na_2CO_3 CaCO_3



grain sizes \sim 100s of microns



Reaction paths and geometry?



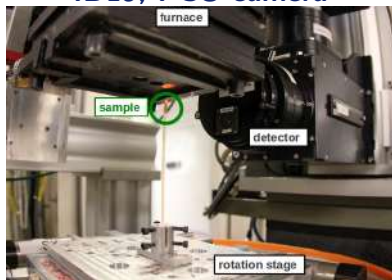
[Chopin et al., 2010]

Large calcium carbonate grains lead to poor quality.

Why?

Tomographic imaging of glass melting

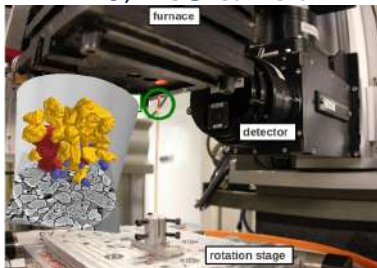
ID19, PCO camera



- Pink beam 19 keV
- Tomo in 1-4 s
- Pixel size of 1.1 μm
- Samples of a few mg
- Furnace : $T \leq 1500^\circ \text{C}$

Tomographic imaging of glass melting

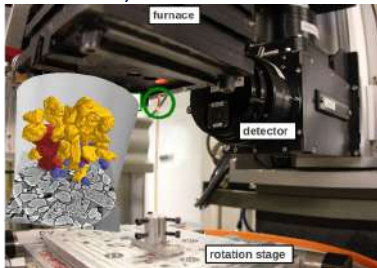
ID19, PCO camera



- Pink beam 19 keV
- Tomo in 1-4 s
- Pixel size of $1.1 \mu\text{m}$
- Samples of a few mg
- Furnace : $T \leq 1500^\circ \text{C}$

Tomographic imaging of glass melting

ID19, PCO camera



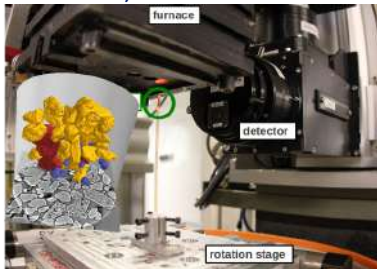
lab tomograph (RX Solutions)



- Pink beam 19 keV
- Tomo in 1-4 s
- Pixel size of $1.1 \mu\text{m}$
- Samples of a few mg
- Furnace : $T \leq 1500^\circ \text{C}$

Tomographic imaging of glass melting

ID19, PCO camera



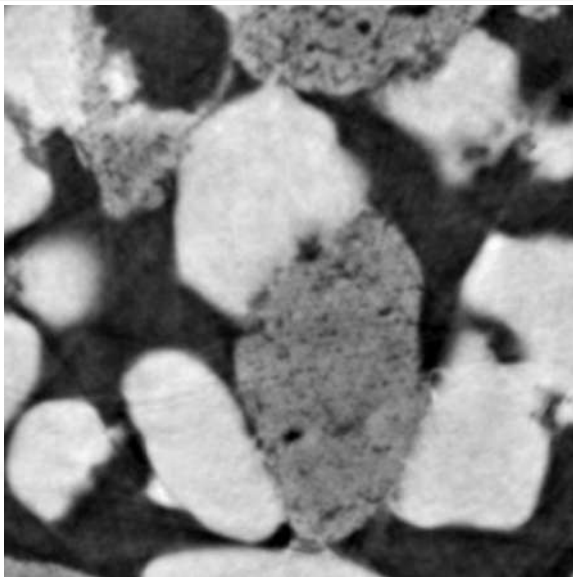
- Pink beam 19 keV
- Tomo in 1-4 s
- Pixel size of $1.1 \mu\text{m}$
- Samples of a few mg
- Furnace : $T \leq 1500^\circ \text{C}$

lab tomograph (RX Solutions)



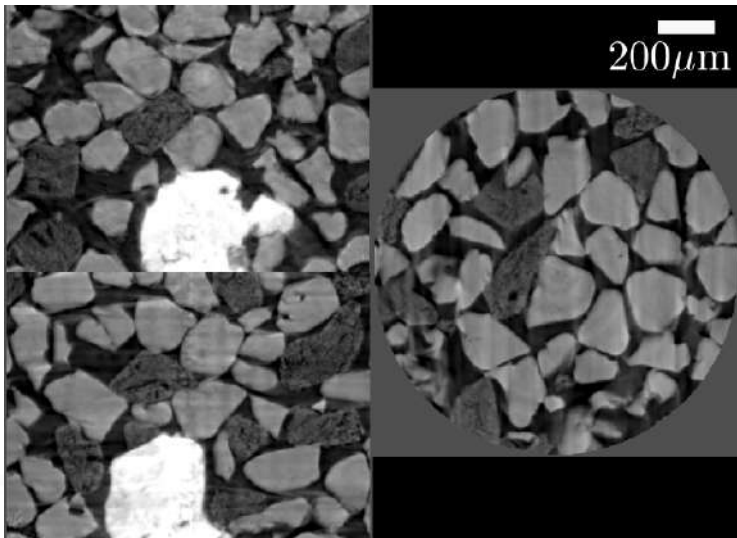
- Polychromatic beam
- Tomo in one hour or more
- Pixel size ≥ 5 microns
- Samples of a few grams

Geometry of solid-state reactions



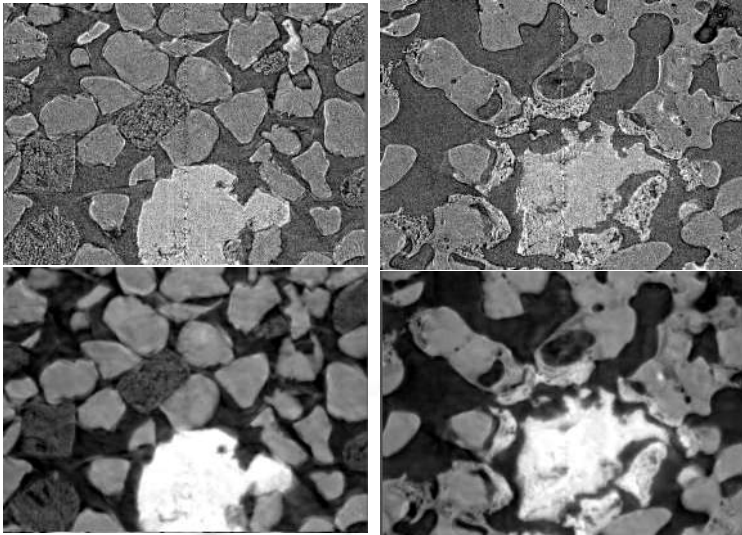
Binary mixture of SiO_2 - Na_2CO_3 , 800°C
[Gouillart et al., 2012], [Grynberg et al., 2015]

The fate of calcium carbonate



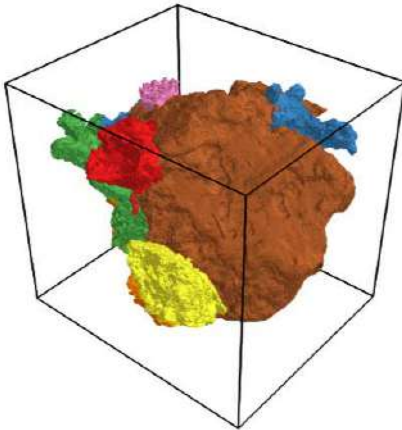
Fast heating at 900°C , ternary mixture of SiO_2 , Na_2CO_3 , CaCO_3

The fate of calcium carbonate



Only outer parts of the grain react
Core of CaO stays unreacted for a long time
Delay in the formation of molten silicates

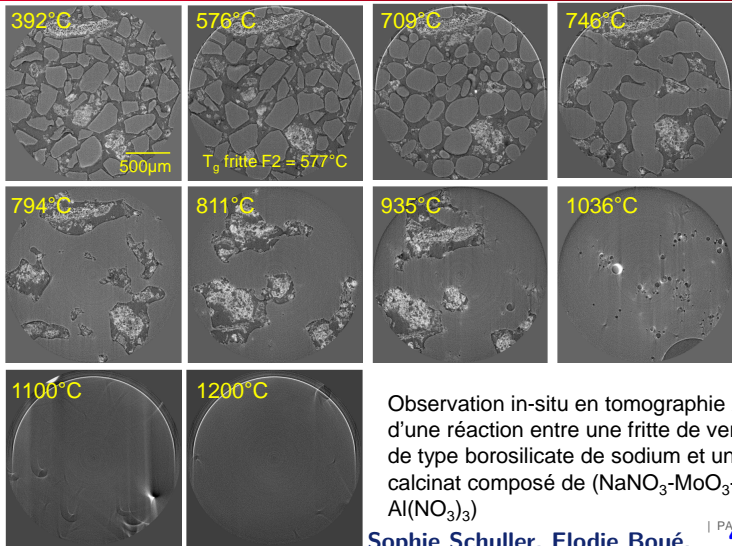
Visualizing the geometry of reactions



Quantifying the reacted parts of the grain



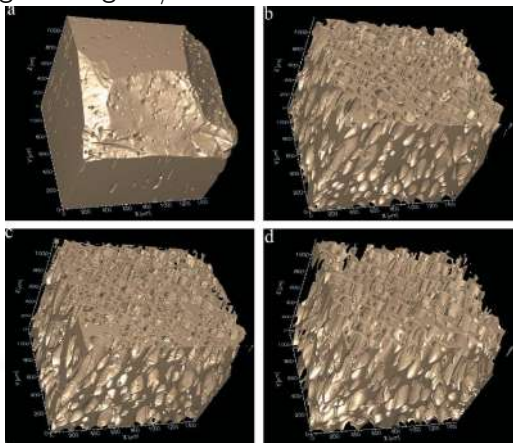
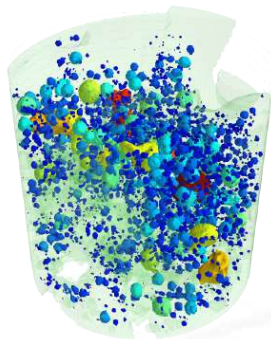
Observation de l'élaboration d'un verre nucléaire de composition simplifiée – microtomographie in situ



Observation in-situ en tomographie X d'une réaction entre une fritte de verre de type borosilicate de sodium et un calcinat composé de $(\text{NaNO}_3\text{-MoO}_3\text{-Al}(\text{NO}_3)_3)$

Bubbles and vesicularity

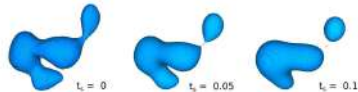
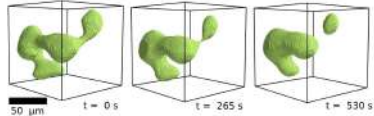
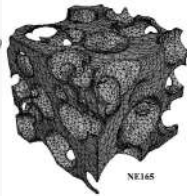
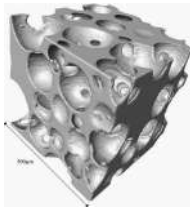
Good contrast between gas and glass/melt



[Fife et al., 2012] : fast heating at $15 \text{ K}\cdot\text{s}^{-1}$ of obsidian glass in range $800 - 1000^\circ\text{C}$.

Ex-solution of water from the melt generates bubbles.

Combination with 3-D modelling



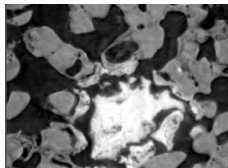
Mechanics : finite-element simulation on mesh determined from tomography
[Youssef et al., 2005]

Estimation of surface tension thanks to hydrodynamic simulations
[Bouttes et al., 2015]

Conclusions

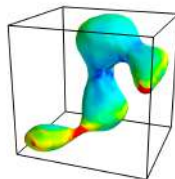
In-situ imaging

- Whole evolution for one sample
- Capture turning points



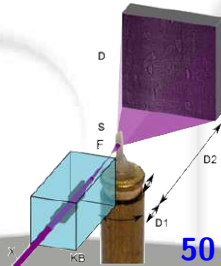
3D imaging

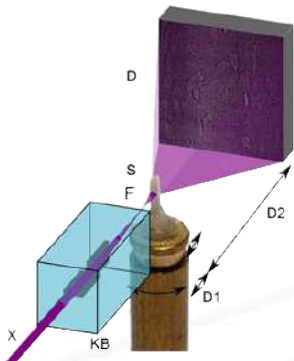
- 3-D information : connectivity, topology
- Whole sample : don't miss where the action is taking place
- More statistics



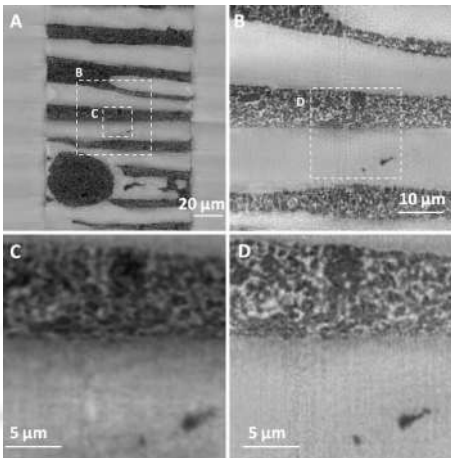
Challenges

- Spatial resolution
- Realistic sample environment
- Data processing
- Link/combine w/ other techniques





ESRF, ID16a

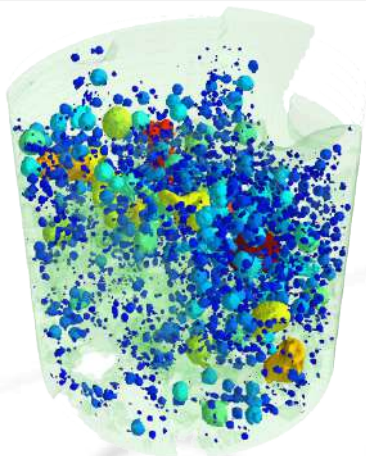
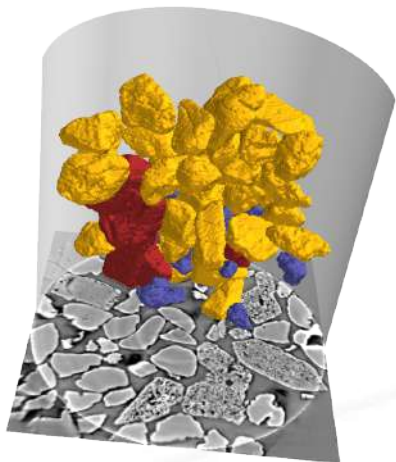


[Villanova et al., 2014]

Acknowledgements

- Synchrotron : Elodie Boller, Alexander Rack, Jean-Paul Valade (ESRF, ID19), Peter Cloetens (ESRF, ID16a), Francesco de Carlo (APS)
- Experiments : David Bouttes, William Woelffel, Damien Vandembroucq, Corinne Claireaux, Emmanuel Garre, Océane Lambert, Luc Salvo, Pierre Lhuissier, Rémi Daudin, Eric Maire, Sophie Schuller, Elise Régnier (and many others)
- Discussions on glass : Marie-Hélène Chopinet, Franck Pigeonneau, Katia Burov, Sophie Papin, Mike Toplis, ...
- Image processing : Hugues Talbot, Gaël Varoquaux, Lionel Moisan
- Funding agencies : Saint-Gobain Recherche, CNRS INP, ANR project EDDAM
- Beamtime : ESRF projects HD501, SC3724, MA1839 and MA1876

Thank you for your attention !



Bibliography I



Bouttes, D., Gouillart, E., Boller, E., Dalmas, D., and Vandembroucq, D. (2014).
Fragmentation and limits to dynamical scaling in viscous coarsening : An interrupted in situ x-ray tomographic study.
Physical review letters, 112(24) :245701.



Bouttes, D., Lambert, O., Claireaux, C., Woelffel, W., Dalmas, D., Gouillart, E., Lhuissier, P., Salvo, L., Boller, E., and Vandembroucq, D. (2015).
Hydrodynamic coarsening in phase-separated silicate melts.
arXiv preprint arXiv :1502.03719.



Chopinnet, M.-H., Gouillart, E., Papin, S., and Toplis, M. J. (2010).
Influence of limestone grain size on glass homogeneity.
Glass Technology-European Journal of Glass Science and Technology Part A, 51(3) :116–122.



Fife, J. L., Rappaz, M., Pistone, M., Celcer, T., Mikuljan, G., and Stampanoni, M. (2012).
Development of a laser-based heating system for in situ synchrotron-based x-ray tomographic microscopy.
Journal of synchrotron radiation, 19(3) :352–358.



Gouillart, E., Toplis, M. J., Grynberg, J., Chopinnet, M.-H., Sondergard, E., Salvo, L., Suéry, M., Di Michiel, M., and Varoquaux, G. (2012).
In situ synchrotron microtomography reveals multiple reaction pathways during soda-lime glass synthesis.
Journal of the American Ceramic Society, 95(5) :1504–1507.



Grynberg, J., Gouillart, E., Chopinnet, M.-H., and Toplis, M. J. (2015).
Importance of the atmosphere on the mechanisms and kinetics of reactions between silica and solid sodium carbonate.
International Journal of Applied Glass Science.

Bibliography II



Kyrieleis, A., Titarenko, V., Ibison, M., Connolley, T., and Withers, P. J. (2011).
Region-of-interest tomography using filtered backprojection : assessing the practical limits.
Journal of Microscopy, 241(1) :69–82.



Leshner, C. E., Wang, Y., Gaudio, S., Clark, A., Nishiyama, N., and Rivers, M. (2009).
Volumetric properties of magnesium silicate glasses and supercooled liquid at high pressure by x-ray
microtomography.
Physics of the Earth and Planetary Interiors, 174(1) :292–301.



Limodin, N., Salvo, L., Boller, E., Suéry, M., Felberbaum, M., Gailliègue, S., and Madi, K. (2009).
In situ and real-time 3-d microtomography investigation of dendritic solidification in an al–10wt.% cu alloy.
Acta Materialia, 57(7) :2300–2310.



Paganin, D., Mayo, S., Gureyev, T. E., Miller, P. R., and Wilkins, S. W. (2002).
Simultaneous phase and amplitude extraction from a single defocused image of a homogeneous object.
Journal of microscopy, 206(1) :33–40.



Slaney, M. and Kak, A. (1988).
Principles of computerized tomographic imaging.
SIAM, Philadelphia.



Terzi, S., Taylor, J., Cho, Y., Salvo, L., Suéry, M., Boller, E., and Dahle, A. (2010).
In situ study of nucleation and growth of the irregular α -al/ β -al 5 fesi eutectic by 3-d synchrotron x-ray
microtomography.
Acta Materialia, 58(16) :5370–5380.

Bibliography III



Villanova, J., Cloetens, P., Suhonen, H., Laurencin, J., Usseglio-Viretta, F., Lay, E., Delette, G., Bleuet, P., Jauffrès, D., Roussel, D., et al. (2014).
Multi-scale 3d imaging of absorbing porous materials for solid oxide fuel cells.
Journal of Materials Science, 49(16) :5626–5634.



Wang, Y., Leshner, C., Fiquet, G., Rivers, M. L., Nishiyama, N., Siebert, J., Roberts, J., Morard, G., Gaudio, S., Clark, A., et al. (2011).
In situ high-pressure and high-temperature x-ray microtomographic imaging during large deformation : A new technique for studying mechanical behavior of multiphase composites.
Geosphere, 7(1) :40–53.



Wang, Y., Rivers, M., Sutton, S., Nishiyama, N., Uchida, T., and Sanehira, T. (2009).
The large-volume high-pressure facility at gsecars : A "swiss-army-knife" approach to synchrotron-based experimental studies.
Physics of the Earth and Planetary Interiors, 174(1) :270–281.



Wang, Y., Uchida, T., Westferro, F., Rivers, M. L., Nishiyama, N., Gebhardt, J., Leshner, C. E., and Sutton, S. R. (2005).
High-pressure x-ray tomography microscope : Synchrotron computed microtomography at high pressure and temperature.
Review of scientific instruments, 76(7) :073709.



Watson, H. C. and Roberts, J. J. (2011).
Connectivity of core forming melts : Experimental constraints from electrical conductivity and x-ray tomography.
Physics of the Earth and Planetary Interiors, 186(3) :172–182.



Weitkamp, T., Haas, D., Wegrzynek, D., and Rack, A. (2012).

Ankaphase : software for single-distance phase retrieval from inline x-ray phase-contrast radiographs.
erratum.

Journal of Synchrotron Radiation, 20(1) :205–205.

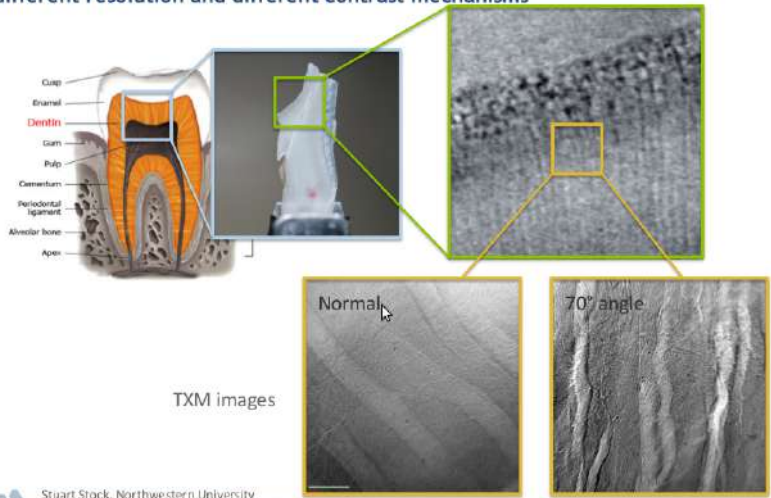


Youssef, S., Maire, E., and Gaertner, R. (2005).

Finite element modelling of the actual structure of cellular materials determined by x-ray tomography.
Acta Materialia, 53(3) :719–730.

Data Fusion Study of Mineralized Tissue

Integration of data from instruments with different resolution and different contrast mechanisms



XTM images